JOC The Journal of Organic Chemistry

Article

pubs.acs.org/joc

Annuloselectivity in Cycloadditions of Ketenes with Imines: A DFT Study

Xinyao Li and Jiaxi Xu*

State Key Laboratory of Chemical Resource Engineering, Department of Organic Chemistry, Faculty of Science, Beijing University of Chemical Technology, 100029 Beijing, People's Republic of China

Supporting Information

ABSTRACT: The annuloselectivity defined as the annulation selectivity between [2 + 2] cycloaddition and two kinds of novel cascade [2 + 2 + 2] cycloadditions (2 ketenes + imine and ketene + 2 imines) in a Staudinger reaction to afford three classes of annulation products has been studied in depth with the density functional theory (DFT) calculations. The computed results indicate that the cascade [2 + 2 + 2] reaction of ketene **4** and ketimine **5** initiates the dimerization of the ketene as the rate-determining step, affording a lactone that further converts to α-acetylketene, followed by the [4 + 2] cycloaddition with imine **5** to furnish a 2,3-dihydro-1,3-oxazin-4-one derivative. That is very competitive to the normal Staudinger reaction. The alternative [2 + 2 + 2] cycloaddition undergoes the hetero-Diels–Alder (HDA) cycloaddition of the zwitterionic intermediates generated from ketenes and conjugated imine **11** with less steric hindrance as a good dienophile to afford 2,3,4,5-tetrahydropyrimidin-6(1*H*)-ones, which is the most favorable pathway in the case of the Staudinger reaction system. The HDA process is supported and confirmed experimentally by X-ray crystallography via analysis of the stereochemistry of the cycloadducts. The further investigation into the nature of the frontier molecular orbitals accounts well for the origin of the annuloselectivity. The extensive studies on ketenes containing various representative substituents reveal that ketenes with electron-donor and conjugated monosubstituents are inclined to dimerization, preferring the [2 + 2 + 2] cycloaddition of two molecules of ketenes and one molecule of imines, while less steric bulky imines with ketenes are apt to the [2 + 2 + 2] cycloaddition of one molecule of ketenes and two molecules of imines.

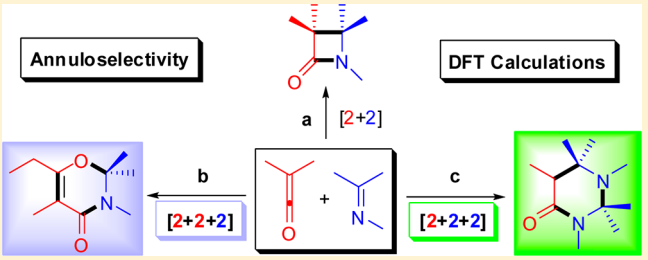

INTRODUCTION

The [2 + 2] cycloaddition reaction of imines and ketenes, referred to as Staudinger reaction or Staudinger cycloaddition,[1] has become one of the most versatile methods for the stereocontrolled synthesis of β-lactams (Scheme 1).[2] Though

Scheme 1. Staudinger Reaction of Ketenes and Imines

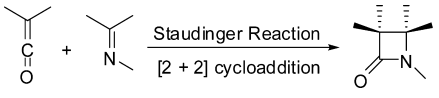

the numerous reports from our laboratory[3] and others[4] have focused on the synthetic methodologies and the diastereoselectivity of β-lactam formation in the Staudinger reaction, there appeared to be some interesting annulation reactions that were found to be fairly general. Among the uncommon reactions, acyl chlorides, as the precursors of ketenes, have now been found to react in different manners (Scheme 2). Bose et al.[5] first proposed that the reaction of acetyl chloride and triethylamine did not give β-lactam with benzalaniline, whereafter Maujean et al.[6] confirmed that an oxazinone derivative instead of β-lactam was generated from a similar reaction. The further experimental study on a hypothesized possibility that implicates the intermediacy of diketene revealed that the [2 + 2 + 2] cycloaddition (2 ketenes + imine) is the most likely pathway. Sohar et al.[7] also reported the experimental observation of the [2 + 2 + 2] cycloaddition of chloroacetyl chloride with an imine. Besides, the formation of spiranic 2,3-dihydro-1,3-oxazin-4-ones derived from arylacetyl chlorides with an imine had been discovered by Arjona et al.[8] in 2002. In our laboratory, the reaction of phenylacetyl chloride with imines via the [2 + 2 + 2] cycloaddition process once again occurred,[9] indicating that the [2 + 2 + 2] cycloaddition of certain acid chlorides and imines is a typical reaction. Recently, Spyroudis and Malamidou-Xenikaki have reported the dimerization of indabedioneketene experimentally,[10] whereafter Bakalbassis with them performed the DFT and MP2 calculations to unravel the mechanism of the dimerization.[11] In addition, dimerization of the parent ketene has also been studied by Dobrowslki using computational methods in 2006.[12] More recently, the related discovery of *N*-heterocyclic carbene-catalyzed formal [2 + 2] and [2 + 2 + 2] cycloadditions of ketenes and isothiocyanates has been encountered by Ye et al.[13]

Alternatively, another [2 + 2 + 2]-type cycloaddition of one molecule of ketenes with two molecules of imines emerges in

Received: October 9, 2012
Published: December 25, 2012

   dx.doi.org/10.1021/jo302216d | *J. Org. Chem.* 2013, 78, 347–355

Scheme 2. Annulation of Two Molecules of Ketenes and One Molecule of Imines

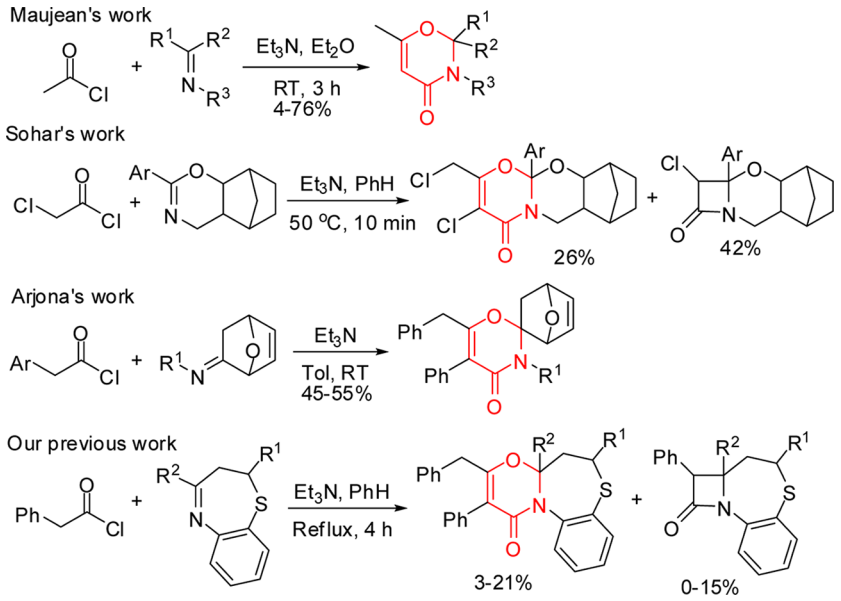

the Staudinger reaction (Scheme 3). Podlech et al.[14] first reported the experimental observation of the [2 + 2 + 2]-

Scheme 3. Annulation of One Molecule of Ketenes and Two Molecules of Imines

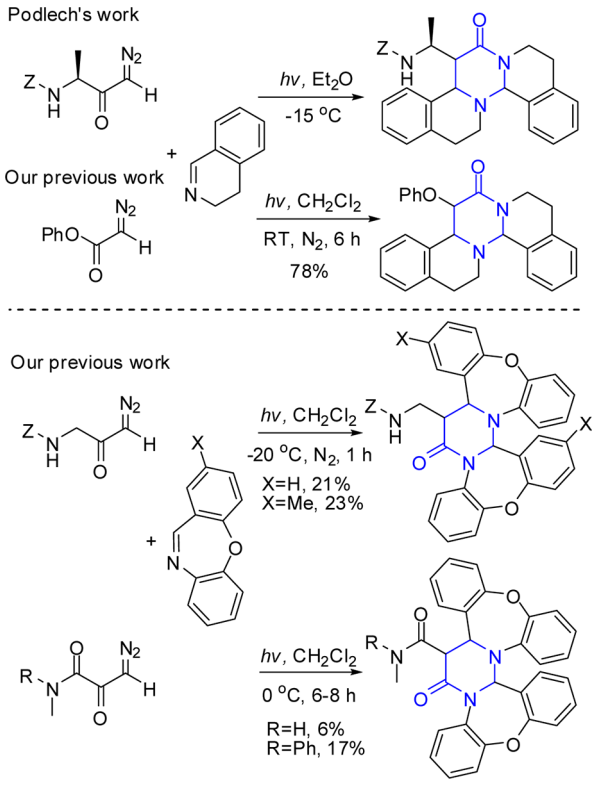

cyclization, affording a pentacycle, with incorporation of a diazoketone ketene precursor and 2 equiv of a cyclic imine under photoirradiation. In recent years, we also encountered the especial annulation of the [2 + 2 + 2] cycloaddition among the Staudinger reaction involving cyclic imines.[3a,h,15]

The [2 + 2] cycloaddition between ketenes and imines has already been extensively explored by DFT, in particular, by Cossío and co-workers;[2f,i] however, to the best of our knowledge, there still lacks a clear mechanistic investigation on the annulation selectivity (annuloselectivity) in cycloaddition of three components. Herein, we report the computational study on the cycloadditions of ketenes and imines, focusing on unraveling the mechanism of the two tandem reactions of [2 + 2 + 2] cycloadditions and in depth comprehending the origin of the annuloselectivity in the Staudinger reactions. We believe that it is critical not only to our mechanistic understanding of the tandem cycloadditions and annuloselectivity but also to guiding the future control and application of the reactions between ketenes and imines in the new synthetic strategies.

COMPUTATIONAL METHODS

All optimized geometries were calculated at the DFT B3LYP level[16] with the 6-311+G(d,p) basis set for all the atoms with the Gaussian 09 suite of programs.[17] Frequency calculations at the B3LYP level at 298 K were performed to confirm each stationary point to be either a minimum or a transition structure. The computed zero-point energies, thermal corrections, and entropies were used for computing enthalpies and free energies. Single-point energies based on the structures obtained at the B3LYP level using the same basis set were obtained by the M06-2X calculations in order to take the dispersion energies into consideration.[18] Solvation energies were evaluated by a self-consistent reaction field (SCRF) using the CPCM model, where UFF radii were used. Solvation calculations were carried out at the M06-2X level on the optimized structures in the gas phase or solution. Where feasible, the DFT data were then validated against benchmark data computed with the high-accuracy CBS-QB3 method.[19] Unless specifically mentioned, all discussed relative energies in this paper are referred to $\Delta G_{sol298K}$. FMO analyses for the cycloaddition were also employed at the HF/6-31G(d) with the former optimized structures.[20] Figures 2 and 4 were prepared using CYLView.[21]

RESULTS AND DISCUSSION

The annuloselectivity in the cycloaddition of ketenes and imines is outlined in Scheme 4. The ketenes and imines with different substituents can proceed through three pathways, one of which is the [2 + 2] cycloaddition via pathway **a**, as the normal Staudinger reaction, and the other two are domino [2 + 2 + 2] cycloadditions via pathways **b** and **c**.

dx.doi.org/10.1021/jo302216d | J. Org. Chem. 2013, 78, 347−355

Scheme 4. Annuloselectivity in Reaction of Ketenes and Imines

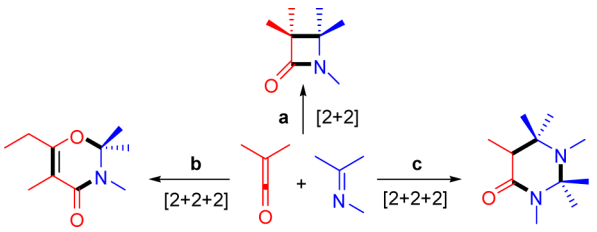

1. [2 + 2] Cycloaddition. The reaction of ketene **1** with imine **2** was selected as the model Staudinger reaction for DFT calculations. The representative potential energy profile of the [2 + 2] cycloaddition reaction as the Staudinger reaction was obtained and is shown in Figure 1. In the first step of the reaction, the imine **2** attacks the ketene **1** to generate a possible zwitterionic intermediate **INT1** via the transition state **TS1** with an activation free energy of 12.7 kcal/mol at the M06-2X(CPCM)//B3LYP(CPCM) level. The second step is a ring closure to form the corresponding β-lactam product **3** via the transition state **TS2**, requiring an activation free energy of 22.2 kcal/mol. For the most Staudinger reactions, the ring-closure step is the rate-determining step, and even the stereo-determining step is amenable to the torquoselectivity theory for the unsymmetric ketenes and imines. Reviewing the whole energy profiles with four theoretical methods, we found that both the B3LYP and M06-2X methods provide similar tendency of the energy profiles although the former one gives the relative energies a little higher. CBS-QB3 was adopted as the standard method for predicting relative energies, and the two M06-2X//B3LYP methods were found to predict relative energies close to those from CBS-QB3. Thus, compared with the results at the CBS-QB3 as a benchmark method, the calculations are considered to be adequate at the M06-2X//B3LYP methods. In addition, these combined methods have been used recently in calculations of cycloadditions by Houk.[22]

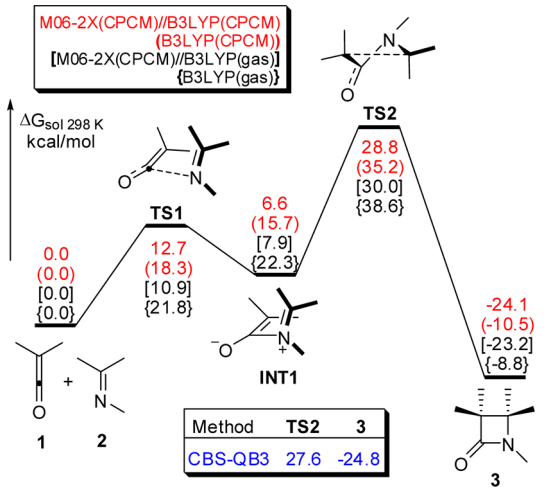

Figure 1. Calculated energy profiles for the [2 + 2] cycloaddition reaction of ketene **1** with imine **2** at the M06-2X and B3LYP levels of theory (CBS-QB3 considered as the benchmark method).

2. [2 + 2 + 2] Cycloaddition of Two Molecules of Ketenes with One Molecule of Imines. The M06-2X- and B3LYP-computed reaction profiles for the simple model of unsubstituted ketene **4** and imine **5** in Maujean's experimental system as the simplified representative model were examined (Figure 2). Normally, ketene **4** and imine **5** can be expected to give rise to the β-lactam **6** through the [2 + 2] ketene−imine cycloaddition. However, the zwitterionic intermediate was not located in gas phase. The [2 + 2] cycloaddition directly undergoes a ring closure, a concerted but significantly asynchronous process as determined by intrinsic reaction coordinate (IRC) analysis of the transition structure, with an activation free energy of 34.1 kcal/mol at the M06-2X-(CPCM)//B3LYP(gas). We next performed optimization calculations in solution and succeeded in getting the transition state **TS3** of the first step and the intermediate **INT2** due to the

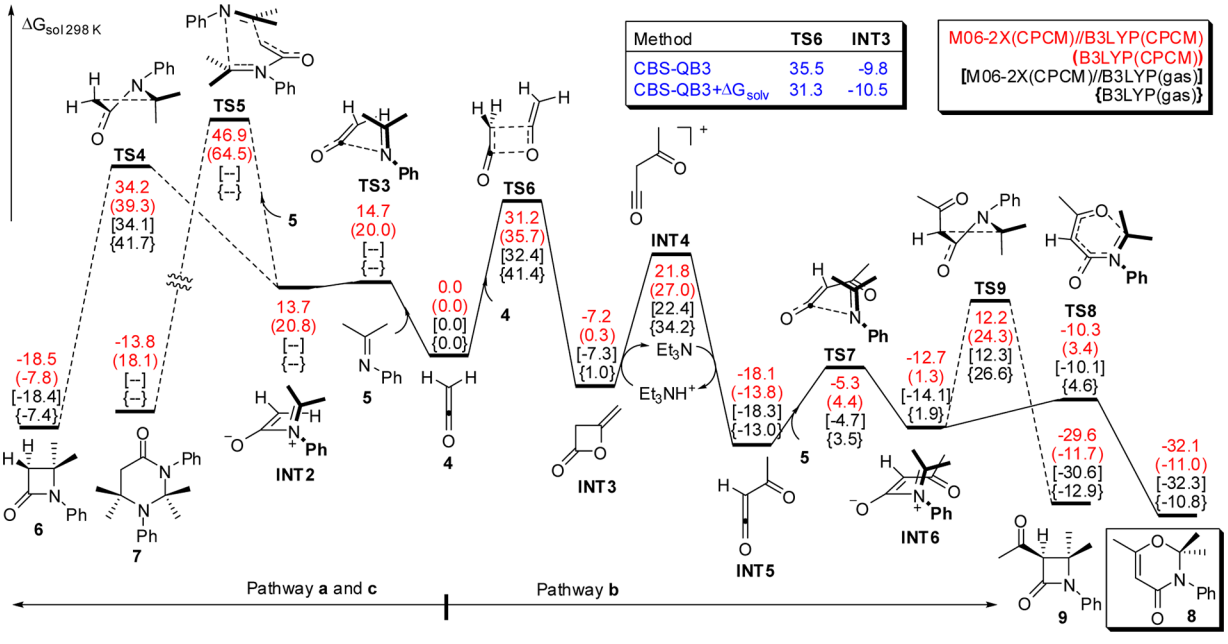

Figure 2. Calculated energy profiles for the [2 + 2 + 2] cycloaddition reaction of ketene **4** with imine **5** at the M06-2X and B3LYP levels of theory (CBS-QB3 considered as the benchmark method).

dx.doi.org/10.1021/jo302216d | J. Org. Chem. 2013, 78, 347−355

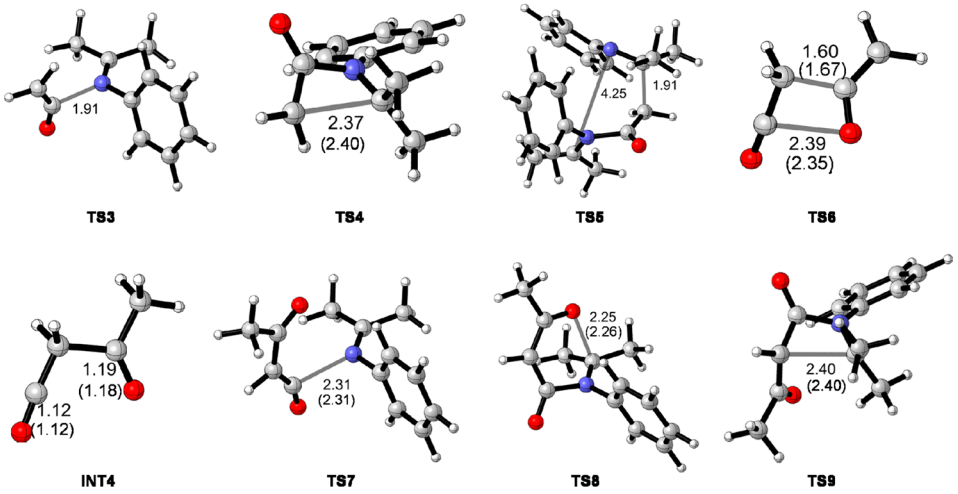

Figure 3. Key species structures in the reaction of ketene **4** and imine **5** optimized at B3LYP(CPCM) in a solution of Et_2O. B3LYP(gas) geometrical parameters are given in parentheses. Selected distances shown in angstroms.

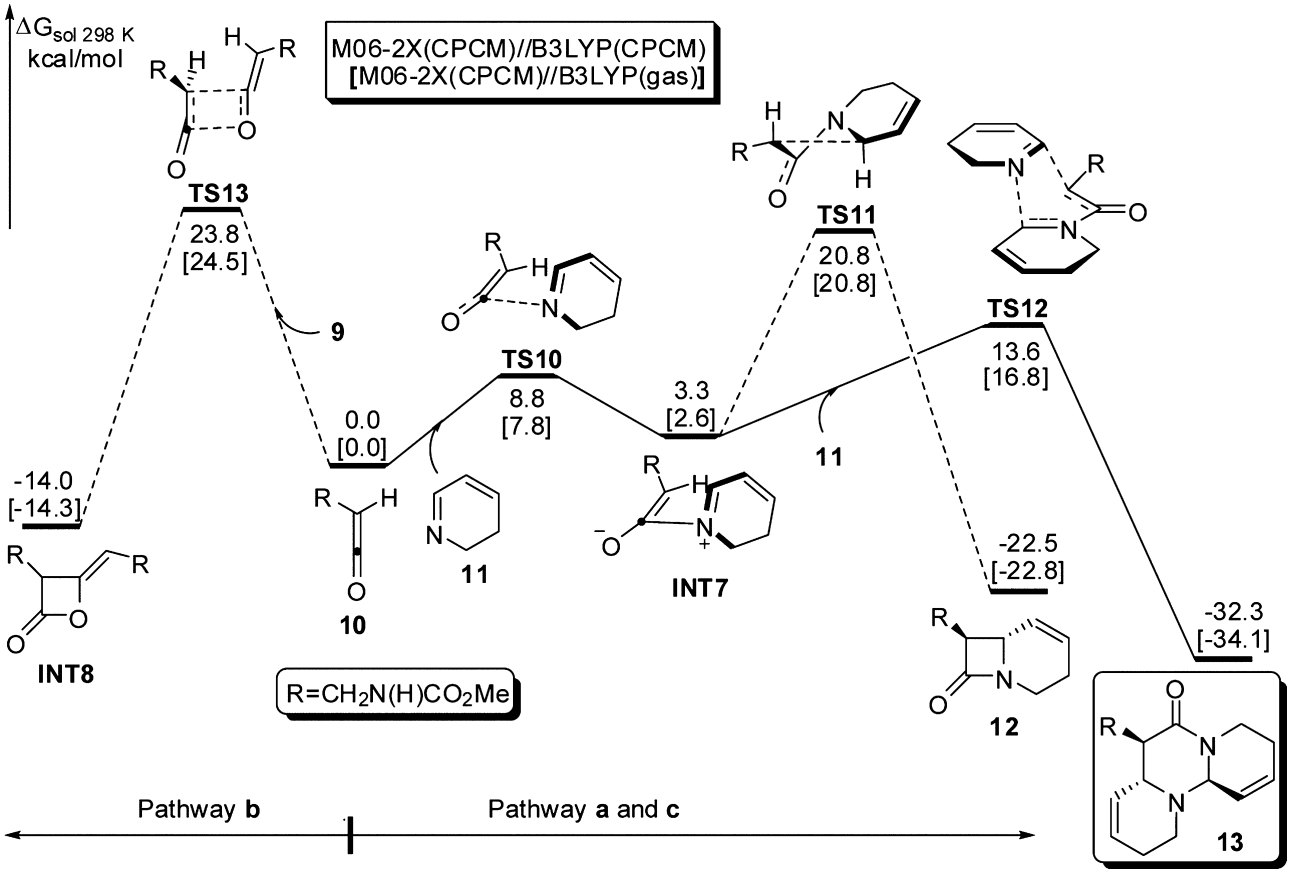

Figure 4. Calculated energy profiles for the [2 + 2 + 2] cycloaddition reaction of ketene **9** with imine **10** at the M06-2X and B3LYP levels of theory.

fact that solvents stabilize **INT2**. Alternatively, **INT2** lies on the energy level close to **TS3** (13.7 vs 14.7 kcal/mol at the M06-2X(CPCM)//B3LYP(CPCM)), indicating that the energy profile of the first step is very flat and the first transition state is located with difficulty. The following ring closure process via **TS4** becomes the rate-determining step with an activation free energy of 34.2 kcal/mol at the M06-2X-(CPCM)//B3LYP(CPCM). In transition state **TS4**, the forming C−C bond distance is 2.40 Å in the gas phase and 2.37 Å in solution (Figure 3).

Alternatively, the [2 + 2 + 2] cycloaddition of 1 equiv of ketene and 2 equiv of imine has been investigated (pathway **c**). The conversion of **INT2** to **7** with another imine **5** passes though **TS5**, in which the forming C−C and C−N bond distances are 1.91 and 4.25 Å, which is viewed as an intermolecular Mannich-like reaction. However, this mechanism suffered from energetic barriers that appeared too high to allow cycloaddition to proceed under the conditions used.

Finally, the [2 + 2 + 2] cycloaddition was also explored with 2 equiv of ketene and 1 equiv of imine. The first step of the

dx.doi.org/10.1021/jo302216d | J. Org. Chem. 2013, 78, 347−355

cascade reaction toward dimerization proceeds via the transition state **TS6** with an activation free energy of 31.2 kcal/mol. In the transition structure, the C−C and C−O bond distances are 1.60 and 2.39 Å, respectively, indicating that the [2 + 2] cycloaddition in the formation of four-membered ring occurs in a concerted but asynchronous fashion (Figure 3). The formation of the lactone **INT3** is slightly exergonic by 7.2 kcal/mol. Protonation of **INT3** with the aid of Et_3NH^+ in situ generated by Et_3N and acyl chloride followed by deprotonation with the aid of Et_3N via **INT4** requires 29.0 kcal/mol in free energy. We did not succeed in getting the TS in this pathway, which seems like a neutralization process.[23] When the lactone **INT3** is converted to α-oxoketene **INT5** with release of the ring strain, the exergonic process lies 18.1 kcal/mol in free energy below the starting materials. The subsequent step is the attack of imine **5** to α-oxoketene **INT5** with an activation free energy of 12.8 kcal/mol. In the transition state **TS6**, the forming N−C bond distance is 2.31 Å in both solution and gas phase. The generation of zwitterionic intermediate **INT6** is slightly exergonic by 7.4 kcal/mol. Finally, the intermediate undergoes ring-closure via a six-membered ring transition state **TS8**, requiring a low activation free energy of 2.4 kcal/mol, to give rise to product **8** that is 32.1 kcal/mol more stable than the starting materials. The forming O−C bond distance in **TS8** is 2.25 Å in solution and 2.26 Å in the gas phase, which is close to that in **INT6** (2.96 Å in solution and 2.90 Å in gas phase), making the pathway facile, while the intermediate can undergo a ring-closure via a four-membered ring transition state **TS9** to give rise to lactam **9**. But the pathway suffers from an energy barrier that appears to be remarkably high and becomes kinetically disfavorable. This is mainly contributed to the four-membered ring strain and notable structure change from **INT6** to **TS9**. The forming C−C bond distance in **TS9** is a bit far from that in **INT6** (3.25 Å in solution and 3.24 Å in gas phase).

Reviewing the whole energy profile, we found that pathway **b** is the most likely to take place to afford lactones **8**, and the rate-determining step of this cascade [2 + 2 + 2] cycloaddition reaction is the dimerization of ketenes, which is very competitive to the direct Staudinger reaction (31.2 vs 34.2 kcal/mol). In addition, the subsequent six-membered ring-closure is facile in relation to the four-membered ring-closure (−10.3 vs 12.2 kcal/mol). These together provide a good interpretation for the experimental observation in the formation of the oxazinones as major products.

Although given the importance of solvation in optimization of **TS3** and **INT2**, there is no obvious difference in structures of other key species such as **TS4**−**9** between those in solution and those in the gas phase. In addition, the relative free energies calculated at the M06-2X(CPCM)//B3LYP(CPCM) level and those at the M06-2X(CPCM)//B3LYP(gas) level are close. Moreover, the two M06-2X//B3LYP were found to predict relative energies close to those from CBS-QB3. Therefore, both of the theoretical methods are considered to be adequate in this system.

3. [2 + 2 + 2] Cycloaddition of One Molecule of Ketenes with Two Molecules of Imines. The potential energy profile for the simple model of ketene **10** and imine **11**, simplified for Podlech's experimental system as to take into consideration the computational efficiency, is shown in Figure 5. Calculations on the model system show that the first step of the cascade reaction corresponds to the attack of imine **11** to ketene **10** to furnish a zwitterionic intermediate **INT7** via the transition state **TS10** with an activation free energy of 8.8 kcal/mol. This is a facile and reversible process. In **TS10**, the forming C−N bond is 2.18 Å in solution and 1.92 Å in gas phase. Subsequently, the second step undergoes a ring closure of four-membered ring with slight energy demand of 20.8 kcal/mol, revealing that the pathway **a** is relatively feasible in this case.

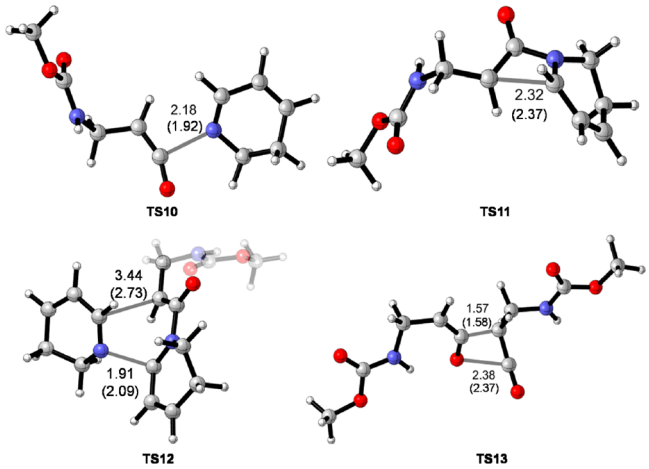

Figure 5. Key transition state structures in the reaction of ketene **10** and imine **11** optimized at B3LYP(CPCM) in a solution of Et_2O. B3LYP(gas) geometrical parameters are given in parentheses. Selected distances shown in angstroms.

Next, the calculation shows an alternative pathway that involves [4 + 2] cycloaddition of the intermediate **INT7** and another imine **11**. It is interesting to disclose that the free energy barrier of the cycloaddition is only 10.3 kcal/mol and the transition state **TS12** is featured in a concerted but asynchronous fashion, since the forming C−C and C−N bond distances are 3.44 and 1.91 Å in solution and 2.73 and 2.09 Å in the gas phase, respectively. Intrinsic reaction coordinate (IRC)[24] calculations were used to confirm the connection between **INT7**, **13**, and **TS12** with any other intermediate, which are given in the Supporting Information. Consequently, the cascade [2 + 2 + 2] cycloaddition is kinetically and thermodynamically favored over the [2 + 2] cycloaddition, leading to the more stable product **13**. After further analyzed the energies, we found that the activation free energy of **TS12** is mainly contributed by the decrease of entropy ($-R\Delta S$) due to the intermolecular reaction, while that of **TS11** primarily arises from the increase of enthalpy (ΔH) because of the ring strain.[25] The competitive pathways are essentially derived from the balance between entropy and enthalpy effects. The reason why **TS12** is favored with respect to **TS11** here is that the less steric hindrance and conjugated imine **11** considered as a good dienophile and the intermediate **7** served as a good diene have little increase of enthalpy (ΔH) to contribute to the increase of free energy (ΔG) in the transition state. By contrary, it is not the case for the steric bulky imine **5**.

After excluding the pathway **a**, we also take into accounting for the pathway **b**, which initially undergoes the dimerization of the ketene as the rate-determining step elucidated by the above discussion. It is found that the dimerization takes place via the **TS13** requiring an activation free energy of 23.8 kcal/mol, which is unfavored by 10.2 kcal/mol in relative to **TS12**. Reviewing the whole energy profile, we noted that the [4 + 2] cycloaddition of intermediate **INT7** and imine **11** is the rate-determining step of the cascade [2 + 2 + 2] cycloaddition. Pathway **c** is remarkably favored over the pathways **a** and **b**,

dx.doi.org/10.1021/jo302216d | J. Org. Chem. 2013, 78, 347−355

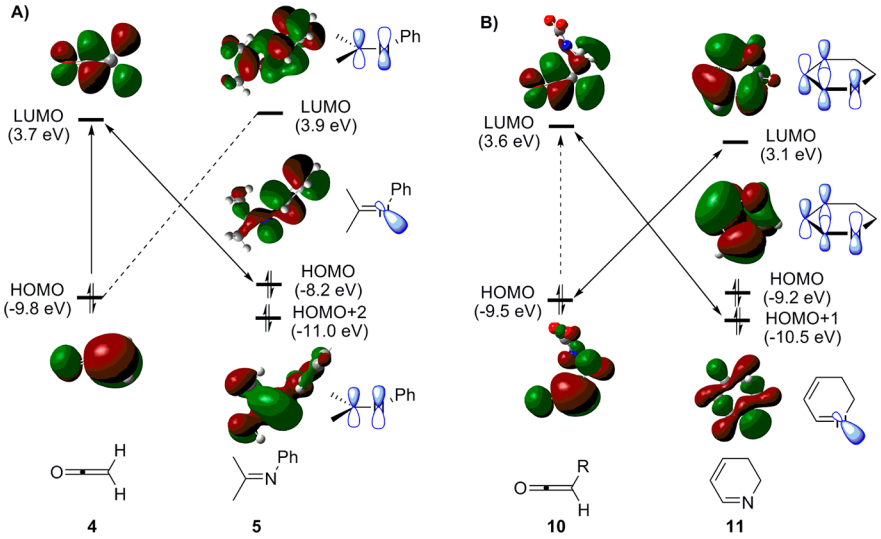

Figure 6. FMOs and orbital energies of ketenes and imines at the HF/6-31G(d) level.

once again in complete accord with the experimental results.[3a,h,15]

For further investigation on the origin of the annuloselectivity in the cycloaddition, the nature of the frontier molecular orbitals (FMOs) of ketenes and imines were explored with the HF method. The FMOs and the energies are shown in Figure 6. The LUMO and HOMO of the parent ketene **4** are mostly localized on the C−C and C−O double bonds, which are well matched during dimerization. The HOMO of imine **5** is mostly localized on the lone pair of electrons on the N atom and the phenyl group. And the HOMO energy lies on the high level (−8.2 eV), leading to the strong nucleophilicity. However, the rate-determining step is the ring closure, which is related to the FMOs of the zwitterionic intermediates derived from the initial attack of the lone pair of electrons in the imine to the ketene. It is notable that the FMOs of the zwitterionic intermediates are the unperturbed HOMO of the ketene and LUMO of the imine (π and π^*, respectively). Therefore, the second step of the Staudinger reaction can also be viewed as an intramolecular Mannich-like reaction, in which the π MO (similar to the HOMO of a ketene) experiences nucleophilic addition on the π^* LUMO, analogous to the LUMO of an imine (Figure 7).[2f] It is interesting to find that the FMO energy gap of dimerization of ketene **4** is slightly smaller than that of the [2 + 2] cycloaddition of **4** and **5**, consistent with the potential energy profile to undergo the pathway **b** involving the dimerization of ketene. FMOs of the substituted ketene **10** resemble closely those of the parent ketene **4**, while FMOs of imine **11** demonstrate different feature in relative to those of imine **5**. It is notable that the HOMO of imine **11** is mostly located on the conjugated π bonds and the HOMO+1 is mainly localized on the lone pair of electrons on the N atom. The LUMO energy lies on the somewhat low level (3.1 eV), resulting in the relatively low FMOs energy gap between the HOMO of **10** and LUMO of **11**. This is in good agreement with the fact that the favored pathway alters to pathway **a** involving the zwitterionic intermediate.

Given its importance as the rate-determining step, the dimerization of ketenes with different substituents and the ring-closure of the [2 + 2] Staudinger reaction were further investigated (Table 1 and Figure 8). The calculational results indicate that ketenes with electron donor groups (entries 1 and

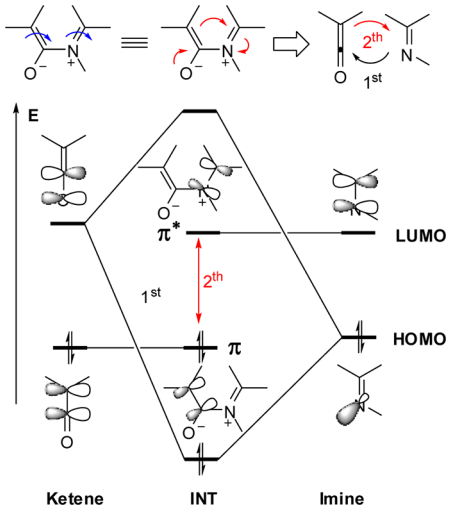

Figure 7. Orbital interaction diagram associated with the formation of the C−N and C−C bonds.

2) and conjugated groups (entries 4 and 5) proceed the dimerization with low activation free energies. However, the energy barriers of the dimerization for both the electron acceptor substituted and disubstituted ketenes appear to be high that the process is difficult to occur (entries 6−9). For the less steric bulky aldimine **A**, [2 + 2] Staudinger reactions are all favorable over the dimerization of ketenes with different substituents. However, when the steric bulky ketimine **B** was used, the parent ketene and methylketene are slightly in favor of the dimerization, while other ketenes still prefer the Staudinger reaction. Therefore, steric hindrance of ketimines retard the [2 + 2] Staudinger reaction of some ketenes, making them dimerization favorable (Figure 8).

The FMOs energies given in Table 1 demonstrate that from alkoxy to parent ketenes, the FMOs energy gaps enhance as well as the free energy barriers for **TS6** (entries 1−3). The phenyl substituent increases the HOMO energy, while the chloro substituent decreases the LUMO energy (entries 4 and 5). When electron-withdrawing groups reduce both FMOs energies with retaining the large gaps, these ketenes are in unfavor of the dimerization (entries 6 and 7). Disubstituted

dx.doi.org/10.1021/jo302216d | J. Org. Chem. 2013, 78, 347−355

Table 1. Dimerization of Ketenes with Different Substituents and Ring Closure of the [2 + 2] Staudinger Reaction[a]

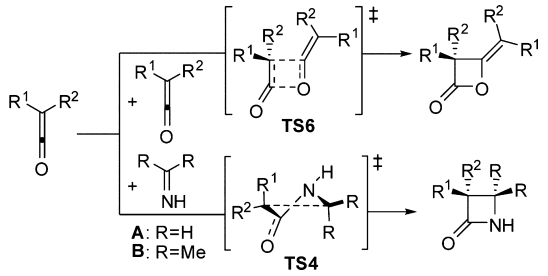

entry	R^1	R^2	LUMO (eV)	HOMO (eV)	$\Delta G^{\ddagger}_{sol}$(**TS6**) (kcal/mol)	$\Delta G^{\ddagger}_{sol}$(**TS4A**) (kcal/mol)	$\Delta G^{\ddagger}_{sol}$(**TS4B**) (kcal/mol)
1	MeO	H	3.2	−9.3	18.0	13.6	16.6
2	Me	H	3.8	−9.3	28.2	27.2	28.8
3	H	H	3.7	−9.8	32.4	32.3	33.3
4	Ph	H	3.3	−8.0	31.0	25.8	26.7
5	Cl	H	2.3	−9.8	22.6	17.4	17.5
6	COMe	H	2.8	−10.3	34.5	31.8	31.2
7	CN	H	2.3	−10.5	36.9	23.8	22.7
8	Me	Me	4.0	−8.9	33.5	31.4	32.6
9	Ph	Me	3.4	−7.8	36.2	30.6	29.5

[a]Orbital energies at the HF level and activation free energies at the M06-2X(CPCM)//B3LYP(gas).

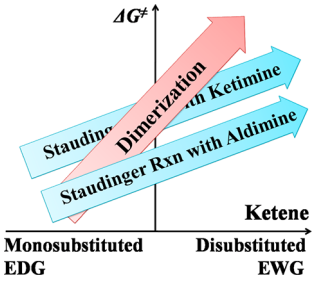

Figure 8. Tendency of the dimerization of ketenes and the ring-closure of the [2 + 2] Staudinger reaction with different substituents.

ketenes have significant steric hindrance effect to impede the dimerization, although they possess small FMOs energy gap (entries 8 and 9).

Ultimately, we sought for the nature of the frontier molecular orbitals for the novel [4 + 2] cycloaddition of intermediate **INT7** and imine **11**. The calculation results shown in Figure 9 suggest that the imine **11** has good FMOs feature of dienophile and the intermediate **INT7** possesses LUMO at low energy level and HOMO at high energy level, considered as a benign diene analogue. Therefore, the [4 + 2] cycloaddition can take place smoothly with the vantage interaction of the FMOs between **INT7** and **11** (10.2 and 9.9 eV). Furthermore, the orbital sizes also match well between the interactional FMOs that render the better orbital overlap in the cycloaddition reaction. Among them, the imine **11** bearing conjugated π bonds as good FMOs feature of dienophile plays an important role in the [4 + 2] cycloaddition. The HDA cycloaddition process is further confirmed experimentally by X-ray crystallography[26] that the stereochemistry of the product structure is consistent with the calculated structure of **13** (Figure 10).

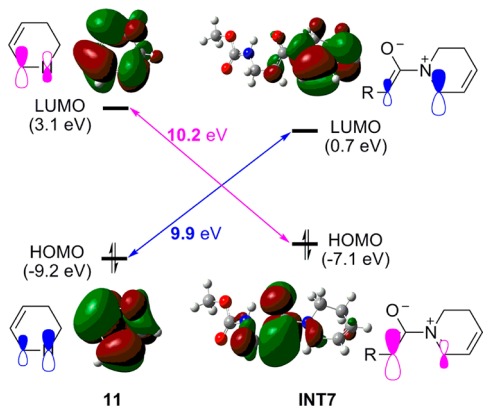

Figure 9. FMOs and orbital energies of imine **11** and intermediate **INT7** at the HF/6-31G(d) level.

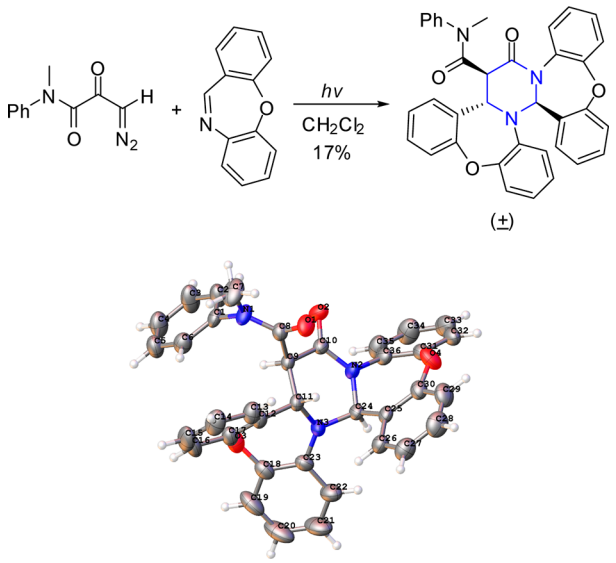

Figure 10. XRD structure of the analogue of **13** (shown with 50% probability ellipsoids).

dx.doi.org/10.1021/jo302216d | J. Org. Chem. 2013, 78, 347−355

CONCLUSIONS

In summary, we have explored the annuloselectivity in the Staudinger reaction of ketenes with imines in three mechanistic possibilities of the [2 + 2] cycloaddition and two kinds of novel cascade [2 + 2 + 2] cycloadditions with the aid of the DFT calculations. The results indicate that, besides the [2 + 2] cycloaddition, monosubstituted ketenes with donor or conjugated groups and ketimines with steric bulky and electron-donating substituents undergo the cascade [2 + 2 + 2] reaction of two molecules of ketenes and one molecule of imine, which initiates the dimerization of ketenes as the rate-determining step, followed by the [4 + 2] cycloaddition with the ketimine to furnish dihydrooxazinone derivatives, that is very competitive to the normal Staudinger reaction, while ketenes and less steric hindrance and conjugated imines take place the alternative [2 + 2 + 2] cycloaddition of one molecule of ketenes and two molecules of imines, in which the conjugated imines with good FMOs feature of dienophile predominantly undergo HDA cycloaddition with the zwitterionic intermediates generated from ketenes and imines to afford tetrahydropyrimidinones. The present computational studies provide comprehensive understanding on the cascade reaction mechanisms and the annuloselectivity, even guide the future application of ketenes and imines in design of new synthetic strategies for heterocyclic compounds.

ASSOCIATED CONTENT

Supporting Information

XRD analysis for the analogue of **13** (CIF) and computational details. This material is available free of charge via the Internet at http://pubs.acs.org.

AUTHOR INFORMATION

Corresponding Author

*Tel: +86-10-6443-5565. Fax: +86-10-6443-5565. E-mail: jxxu@mail.buct.edu.cn.

Notes

The authors declare no competing financial interest.

ACKNOWLEDGMENTS

The project was supported by the National Natural Science Foundation of China (Nos. 21172017, 20972013 and 20772005), the specialized Research Fund for the Doctoral Program of Higher Education, Ministry of Education of China (No. 20110010110011), and "CHEMCLOUDCOMPUTING" of Beijing University of Chemical Technology.

REFERENCES

(1) Staudinger, H. *Justus Liebigs Ann. Chem.* **1907**, *356*, 51.
(2) (a) *The Organic Chemistry of β-Lactams*; Georg, G. I., Ed.; Verlag Chemie: New York, 1993. (b) Palomo, C.; Aizpurua, J. M.; Ganboa, I.; Oiarbide, M. *Eur. J. Org. Chem.* **1999**, 3223. (c) Singh, G. S. *Tetrahedron* **2003**, *59*, 7631. (d) Palomo, C.; Aizpurua, J. M.; Ganboa, I.; Oiarbide, M. *Curr. Med. Chem.* **2004**, *11*, 1837. (e) Alcaide, B.; Almendros, P.; Aragoncillo, C. *Chem. Rev.* **2007**, *107*, 4437. (f) Cossío, F. P.; Arrieta, A.; Sierra, M. A. *Acc. Chem. Res.* **2008**, *41*, 925. (g) Brandi, A.; Cicchi, S.; Cordero, F. M. *Chem. Rev.* **2008**, *108*, 3988. (h) Fu, N. Y.; Tidwell, T. T. *Tetrahedron* **2008**, *64*, 10465. (i) Arrieta, A.; Lecea, B.; Cossío, F. P. *Top. Heterocycl. Chem.* **2010**, 313. (j) Xu, J. X. *Tetrahedron* **2012**, *68*, 10696.
(3) (a) Liang, Y.; Jiao, L.; Zhang, S. W.; Xu, J. X. *J. Org. Chem.* **2005**, *70*, 334. (b) Jiao, L.; Liang, Y.; Xu, J. X. *J. Am. Chem. Soc.* **2006**, *128*, 6060. (c) Jiao, L.; Liang, Y.; Zhang, Q. F.; Zhang, S. W.; Xu, J. X. *Synthesis* **2006**, 659. (d) Wang, Y. K.; Liang, Y.; Jiao, L.; Du, D.-M.; Xu, J. X. *J. Org. Chem.* **2006**, *71*, 6983. (e) Li, B. N.; Wang, Y. K.; Du, D.-M.; Xu, J. X. *J. Org. Chem.* **2007**, *72*, 990. (f) Hu, L. B.; Wang, Y. K.; Li, B. N.; Du, D.-M.; Xu, J. X. *Tetrahedron* **2007**, *63*, 9387. (g) Liang, Y.; Jiao, L.; Zhang, S. W.; Yu, Z. X.; Xu, J. X. *J. Am. Chem. Soc.* **2009**, *131*, 1542. (h) Qi, H. Z.; Li, X. Y.; Xu, J. X. *Org. Biomol. Chem.* **2011**, *9*, 2702. (i) Wang, Z. X.; Chen, N.; Xu, J. X. *Tetrahedron* **2011**, *67*, 9690.
(4) (a) Moore, H. W.; Hernandez, L. J.; Chambers, R. *J. Am. Chem. Soc.* **1978**, *100*, 2245. (b) Pacansky, J.; Chang, J. S.; Brown, D. W.; Schwarz, W. *J. Org. Chem.* **1982**, *47*, 2233. (c) Moore, H. W.; Hughes, G.; Srinivasachar, K.; Fernandez, M.; Nguyen, N. V.; Schoon, D.; Tranne, A. *J. Org. Chem.* **1985**, *50*, 4231. (d) Brady, W. T.; Gu, Y. Q. *J. Org. Chem.* **1989**, *54*, 2838. (e) Lynch, J. E.; Riseman, S. M.; Laswell, W. L.; Tschaen, D. M.; Volante, R.; Smith, G. B.; Shinkai, I. *J. Org. Chem.* **1989**, *54*, 3792. (f) Hegedus, L. S.; Montgomery, J.; Narukawa, Y.; Snustad, D. C. *J. Am. Chem. Soc.* **1991**, *113*, 5784. (g) Georg, G. I.; He, P.; Kant, J.; Wu, Z. J. *J. Org. Chem.* **1993**, *58*, 5771. (h) Alcaide, B.; Almendros, P.; Salgado, N. R.; Rodríguez-Vicente, A. *J. Org. Chem.* **2000**, *65*, 4453.
(5) Bose, K.; Splegelman, G.; Manhas, M. S. *Tetrahedron Lett.* **1971**, 3167.
(6) Maujean, A.; Chuche, J. *Tetrahedron Lett.* **1976**, 2905.
(7) Sohár, P.; Stájer, G.; Pelczer, I.; Szabó, A. E.; Szúnyog, J.; Bernáth, G. *Tetrahedron* **1985**, *41*, 1721.
(8) Arjona, O.; Csákÿ, A. G.; Murcia, M. C.; Plumet, J. *Tetrahedron Lett.* **2002**, *43*, 6405.
(9) Xu, J. X.; Wang, C.; Zhang, Q. H. *Chin. J. Chem.* **2004**, *22*, 1012.
(10) (a) Koulouri, S.; Malamidou-Xenikaki, E.; Spyroudis, S.; Tsanakopoulou, M. *J. Org. Chem.* **2005**, *70*, 8780. (b) Malamidou-Xenikaki, E.; Spyroudis, S.; Tsanakopoulou, M.; Krautscheid, H. *J. Org. Chem.* **2007**, *72*, 502.
(11) (a) Bakalbassis, E. G.; Spyroudis, S.; Tsiotra, E. *J. Org. Chem.* **2006**, *71*, 7060. (b) Bakalbassis, E. G.; Malamidou-Xenikaki, E.; Spyroudis, S.; Xantheas, S. S. *J. Org. Chem.* **2010**, *75*, 5499.
(12) Rode, J. E.; Dobrowolski, J. C. *J. Phys. Chem. A* **2006**, *110*, 207.
(13) Wang, X.-N.; Shen, L.-T.; Ye, S. *Org. Lett.* **2011**, *13*, 6382.
(14) Linder, M. R.; Frey, W. U.; Podlech, J. *J. Chem. Soc., Perkin Trans. 1* **2001**, 2566.
(15) Qi, H. Z.; Yang, Z. H.; Xu, J. X. *Synthesis* **2011**, 723.
(16) (a) Becke, A. D. *J. Chem. Phys.* **1993**, *98*, 5648. (b) Lee, C.; Yang, W.; Parr, R. G. *Phys. Rev. B* **1988**, *37*, 785.
(17) Gaussian 09, Revision B.01: Frisch, M. J.; Trucks, G. W.; Schlegel, H. B.; Scuseria, G. E.; Robb, M. A.; Cheeseman, J. R.; Scalmani, G.; Barone, V.; Mennucci, B.; Petersson, G. A.; Nakatsuji, H.; Caricato, M.; Li, X.; Hratchian, H. P.; Izmaylov, A. F.; Bloino, J.; Zheng, G.; Sonnenberg, J. L.; Hada, M.; Ehara, M.; Toyota, K.; Fukuda, R.; Hasegawa, J.; Ishida, M.; Nakajima, T.; Honda, Y.; Kitao, O.; Nakai, H.; Vreven, T.; Montgomery, J. A., Jr.; Peralta, J. E.; Ogliaro, F.; Bearpark, M.; Heyd, J. J.; Brothers, E.; Kudin, K. N.; Staroverov, V. N.; Kobayashi, R.; Normand, J.; Raghavachari, K.; Rendell, A.; Burant, J. C.; Iyengar, S. S.; Tomasi, J.; Cossi, M.; Rega, N.; Millam, J. M.; Klene, M.; Knox, J. E.; Cross, J. B.; Bakken, V.; Adamo, C.; Jaramillo, J.; Gomperts, R.; Stratmann, R. E.; Yazyev, O.; Austin, A. J.; Cammi, R.; Pomelli, C.; Ochterski, J. W.; Martin, R. L.; Morokuma, K.; Zakrzewski, V. G.; Voth, G. A.; Salvador, P.; Dannenberg, J. J.; Dapprich, S.; Daniels, A. D.; Farkas, Ö.; Foresman, J. B.; Ortiz, J. V.; Cioslowski, J.; Fox, D. J. Gaussian, Inc., Wallingford, CT, 2009.
(18) Zhao, Y.; Truhlar, D. G. *Theor. Chem. Acc.* **2008**, *120*, 215.
(19) (a) Montgomery, J. A., Jr.; Frisch, M. J.; Ochterski, J. W.; Petersson, G. A. *J. Chem. Phys.* **1999**, *110*, 2822. (b) Montgomery, J. A., Jr.; Frisch, M. J.; Ochterski, J. W.; Petersson, G. A. *J. Chem. Phys.* **2000**, *112*, 6532.
(20) French, A. D.; Kelterer, A.-M.; Johnson, G. P.; Dowd, M. K.; Cramer, C. J. *J. Comput. Chem.* **2001**, *22*, 65.
(21) Legault, B. Y. CYLView, 1.0b; Université de Sherbrooke: Québec, Montreal, Canada, 2009; http://www.cylview.org.

(22) (a) Pham, H. V.; Martin, D. B. C.; Vanderwal, C. D.; Houk, K. N. *Chem. Sci.* **2012**, 3, 1650. (b) Lan, Y.; Danheiser, R. L.; Houk, K. N. *J. Org. Chem.* **2012**, *77*, 1533.

(23) Two pathways were proposed for the transformation of **INT3** into **INT5** with the assistance of Et_3N. When the first step is deprotonation of **INT3** by Et_3N, we succeed in getting a transition state **TS3−5**. But this pathway was ruled out due to the high energetic barrier of 48.9 kcal/mol. Thus, the conversion of **INT3** into **INT5** via **INT4** is most likely to occur.

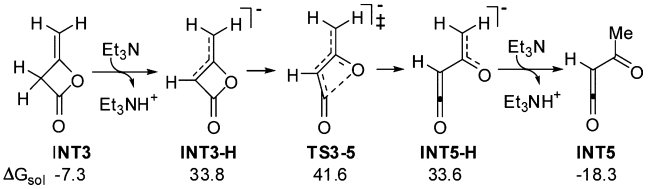

(24) (a) Fukui, K. *J. Phys. Chem.* **1970**, *74*, 4161. (b) Ishida, K.; Morokuma, K.; Komornicki, A. *J. Chem. Phys.* **1977**, *66*, 2153. (c) González, C.; Schlegel, H. B. *J. Phys. Chem.* **1990**, *94*, 5523.

(25) The activation free energy of **TS12** is mainly contributed by the decrease of entropy ($-R\Delta S$), while that of **TS11** primarily arises from the increase of enthalpy (ΔH).

M06-2X	**INT7**	**TS11**	**TS12**
ΔG_{sol}	2.6	20.8	16.8
ΔH_{sol}	−10.3	6.1	−10.0
$-R\Delta S$	12.9	14.7	26.8

(26) Single crystals of $C_{36}H_{27}N_3O_4$ (analogue of **13**) were recrystallized from a mixture of petroluem ether, and ethyl acetate A crystal was selected and mounted in inert oil and transferred to a diffractometer with a cold gas stream. **Crystal Data:** $C_{36}H_{27}N_3O_4$, M = 565.61, monoclinic, space group $P2_1/n$ (no. 14), a = 9.9283(6) Å, b = 17.019(2) Å, c = 16.7464(10) Å, β = 96.924(5)°, U = 2809.0(5) Å^3, Z = 4, T = 293(2), μ(Mo Kα) = 0.088, 12678 reflections measured, 5506 unique (R_{int} = 0.0326) which were used in all calculations. The final w$R(F_2)$ was 0.1105 (all data).

dx.doi.org/10.1021/jo302216d | *J. Org. Chem.* 2013, 78, 347−355